

## MODEL-BASED ESTIMATION OF WIND FIELDS OVER THE OCEAN FROM WIND SCATTEROMETER MEASUREMENTS

D G Long & J M Mendel

University of Southern California  
Los Angeles, California

### ABSTRACT

A wind scatterometer is a radar remote sensing instrument which measures the wind-dependent radar backscatter of the ocean's surface. From these measurements the near-surface wind over the ocean can be inferred. We introduce a model-based approach to estimating the entire wind field over the swath simultaneously. This fundamentally new approach incorporates dynamical constraints provided by a mathematical model of the wind field and eliminates the "dealiasing" required in traditional wind retrieval process. The new approach results in more accurate wind estimates and the ability to quantify the accuracy of the resulting wind field estimates. This paper summarizes the development of the wind field model and provides an illustrative comparison of the model-based and traditional wind estimation schemes.

**Keywords:** scatterometer, winds, estimation

### 1. INTRODUCTION

In the mid 1980's the NASA-sponsored experimental satellite known as SEASAT demonstrated, among other things, that winds over the ocean could be measured from space using a wind scatterometer (Refs. 15,7). The scatterometer measures the wind-dependent radar backscatter of the ocean's surface from which the speed and direction of the wind over the ocean's surface is estimated. Unfortunately, the point-wise estimation procedure traditionally used results in non-unique estimates of the wind vector. Since a single estimate of the wind is required for most oceanographic and meteorological studies, the ambiguity in the wind vector estimate is resolved using an error-prone "dealiasing" step to select a unique wind field map (Ref. 14).

The purpose of this paper is to introduce an estimation-theory based approach to estimating the wind vector field; it uses a model, based on fundamental physical principles, for the underlying wind field. In the proposed approach, the noisy wind scatterometer measurements are used to estimate the parameters of the wind field model. The wind field estimate is then computed using the model parameters. This approach is fundamentally different from the traditional point-wise approach to wind field estimation. It eliminates the "dealiasing" step and yields more accurate estimates of the wind field. While the approach is computationally intensive, the model-based wind field estimation technique permits analysis of the accuracy of the wind field measurement. This can be very difficult using the traditional approach due to the *ad hoc* nature of the dealiasing step.

An outline of this paper is as follows. First, background information is provided, followed by a brief description of the traditional estimation approach. We then present a mathematical development of a very simple *descriptive* wind field model. The resulting estimation problem is formulated and simulated results are presented and compared with the more traditional point-wise wind field estimates.

### 2. BACKGROUND

The normalized radar backscatter ( $\sigma^\circ$ ) (at Ku band) of the ocean's surface depends on the wind speed and the relative az-

imuth angle between the radar illumination and the wind direction in a manner which varies with the incidence angle of the radar on the ocean surface and the radar polarization (Refs. 15,4). The relationship between  $\sigma^\circ$  and the wind is known as the *geophysical model function* and will be denoted by  $\mathcal{M}$ . A typical example of  $\mathcal{M}$  is the SASS-I model function which relates  $\sigma^\circ$  to the neutral stability wind at 19.5 m (Ref. 4).

Since  $\mathcal{M}$  has a multi-valued inverse, several measurements of  $\sigma^\circ$  from different azimuth angles are used to infer the wind. The SeaSat scatterometer obtained  $\sigma^\circ$  measurements from only two azimuth angles on an irregular sampling grid. Second-generation scatterometers such as NSCAT (Ref. 11) will obtain  $\sigma^\circ$  measurements from 3 or more azimuth angles on an equally-spaced grid of sample points over the measurement swath. These noisy measurements of  $\sigma^\circ$  provide an essentially instantaneous sample of the wind field across the swath over the ocean's surface. The problem is to estimate the original wind field at the sample points from the noisy  $\sigma^\circ$  measurements.

### 3. POINT-WISE WIND ESTIMATION

In the traditional approach, the noisy  $\sigma^\circ$  measurements are used in a point-wise estimation scheme in which only the  $\sigma^\circ$  measurements for a given grid cell are used to estimate the wind for that cell. An objective function (typically based on the likelihood function) formulated using the noisy  $\sigma^\circ$  measurements, is minimized with respect to the wind speed and direction at the sample point. Unfortunately, due to the nature of  $\mathcal{M}$ , the objective function is minimized by several wind vectors. This approach is unable to uniquely estimate the wind vector and several ambiguous wind estimates result for each cell. The multiple estimates are termed *ambiguities* or *aliases* (Ref. 14). To select a single wind estimate for each cell, a post-estimation procedure known in the literature as "dealiasing" or "ambiguity removal" is used (Refs. 14,16). Dealiasing procedures have used various *ad hoc* measures and/or pattern recognition of significant weather features to select a wind vector at each sample point of the wind field (Refs. 14,16). More recently, dealiasing based on dynamical considerations for the resultant wind field with data assimilation techniques has been studied (Refs. 2,9,10). Dealiasing is prone to large systematic errors (Refs. 1,14,16).

### 4. MODEL-BASED WIND FIELD ESTIMATION

Rather than using the traditional point-wise approach to wind estimation, we propose using a model-based estimation procedure to estimate the entire wind field over the measurement swath. This new approach eliminates the need for dealiasing and provides more accurate wind field estimates by taking advantage of the inherent correlation in the wind between different sample points. In this approach we formulate an objective function based on the likelihood function for the model parameters using the noisy  $\sigma^\circ$  measurements. The model parameters are estimated by minimizing the objective function. Finally, the estimated wind field is computed from the model parameters. In effect, this procedure permits us to estimate the entire wind field simultaneously.

For model-based wind field estimation a mathematical model for describing and/or representing the wind field for the purposes

of wind estimation is needed. The wind field model must be capable of representing near-surface mesoscale wind fields. Since other data sources are not always available, we require that the model use only scatterometer data. To be useful for wind field estimation, the model must be computationally tractable and lend itself to a model parameter estimation formulation. Note that while we will base the model formulation on physical principles, the model does not necessarily have to be based on atmospheric dynamics since the model is used only for describing a snapshot of the near-surface wind field and not for propagating winds.

In this paper we present a particularly simple wind field model based on the geostrophic equation and rather simplistic assumptions regarding the divergence and curl of the wind field, which is adequate for use in wind field estimation. As part of our continuing research we are investigating more sophisticated models.

### 5. THE WIND FIELD MODEL

The wind field model provides a description of the wind field over the scatterometer measurement swath at a fixed instant of time and a resolution of 25 km (corresponding to the scatterometer sampling). To simplify matters we restrict our attention to limited-area regions with a maximum spatial extent of approximately 600 km (Ref. 11).

Denote the near-surface horizontal wind field of interest by  $\mathbf{U} = (u, v)^T$ . We are interested in a mathematical model providing a reasonably accurate description of  $\mathbf{U}$  over a (limited-area) region  $\mathcal{L}$ . The vorticity  $\zeta$  and divergence  $\delta$  of  $\mathbf{U}$  are defined, as

$$\zeta = \mathbf{k} \cdot \nabla \times \mathbf{U} \quad (1)$$

$$\delta = \nabla \cdot \mathbf{U} \quad (2)$$

Using the Helmholtz theorem,  $\mathbf{U}$  may be defined by a streamfunction  $\psi$  and velocity potential  $\chi$ , according to

$$\mathbf{U} = \mathbf{k} \times \nabla \psi + \nabla \chi \quad (3)$$

where  $\mathbf{k} \times \nabla \psi$  is a nondivergent vector field and  $\nabla \chi$  is a curl-free vector field (Ref. 3).

Taking the divergence and curl, respectively, of Eq. (3) we obtain Poisson equations for  $\psi$  and  $\chi$  (Ref. 13),

$$\nabla^2 \psi = \zeta \quad (4)$$

$$\nabla^2 \chi = \delta \quad (5)$$

These equations appear in the classic problems of partitioning a given wind field into its rotational and non-divergent components and reconstructing a wind field from specified vorticity and divergence (Refs. 3,13). For this latter problem, Lynch (Ref. 13) argues that the reconstruction is not unique over a limited domain; an arbitrary harmonic function may be added to  $\chi$ , provided  $\psi$  is also altered, to produce the same wind field. From this he concludes that the boundary values of  $\chi$  may be set arbitrarily. He shows that setting the boundary values of  $\chi$  to zero minimizes the divergent component of the kinetic energy. Choosing  $\chi = 0$  on the boundary ensures a unique reconstruction of the wind field.

Following this line of reasoning, our *first* modeling assumption is to assume that  $\chi = 0$  on the region boundary. This corresponds to wind fields with minimum divergent kinetic energy. Assuming that  $\chi = 0$  on the boundary, Eqs. (4) and (5), the vorticity and divergence fields and the boundary conditions for  $\psi$ , are sufficient for describing the wind vector field.

To obtain simple boundary conditions we make a *second* major modeling assumption by attributing  $\psi$  to the geostrophic motion. This second assumption is that the streamfunction  $\psi$  is proportional to the geostrophic pressure field  $p$ ,

$$\psi = \frac{1}{\rho_s f} p \quad (6)$$

where  $\rho_s$  is the density and  $f$  is the Coriolis parameter. Note that in a strictly geostrophic formulation, the wind field would be non-divergent and  $\chi$  would be identically zero. In the more general formulation which we will adopt,  $\chi$  corresponds to the *ageostrophic* component of the wind. This generalization allows us to apply the model to mesoscale wind fields which depart from strict geostrophy. Inclusion of the ageostrophic flow permits the model to span a wider space in describing the wind field. Note that  $\psi$  and  $\chi$  will be derived from the observed wind field.

By making assumption two, the boundary values for Eqs. (4) and (5) can be specified in terms of the geostrophic pressure field. This avoids the difficulties of using velocity boundary conditions

which may yield an overdetermined system (Ref. 13).

Our *third* modeling assumption is that over the region of interest  $\rho_s f$  is essentially constant (i.e., an *f*-plane approximation); we do this to simplify the mathematics. We can then normalize the pressure field by  $\rho_s f$  so that  $\psi = p$ , i.e.,  $\psi$  is then the normalized geostrophic pressure field. Using this definition, Eq. (3) can be written in component form as,

$$u = -\frac{\partial p}{\partial y} + \frac{\partial \chi}{\partial x} \quad (7)$$

$$v = \frac{\partial p}{\partial x} + \frac{\partial \chi}{\partial y} \quad (8)$$

These two equations, along with Eqs. (4) and (5) form the basis of our wind field model.

To complete the wind field model, descriptions of the vorticity and divergence fields are needed. Our *fourth* and final assumption is that the vorticity and divergence fields are relatively smooth and can be adequately modeled by low-order bivariate polynomials over the region of interest. Note that the coefficients of the polynomials will be derived from the observed wind fields. In this paper, we have assumed the following bivariate forms for the vorticity and divergence fields,

$$\zeta(x, y) = \sum_{m=0}^{M_C} \sum_{\substack{n=0 \\ m+n \leq M_C}}^{M_C} c_{m,n} x^m y^n \quad (9)$$

$$\delta(x, y) = \sum_{m=0}^{M_D} \sum_{\substack{n=0 \\ m+n \leq M_D}}^{M_D} d_{m,n} x^m y^n \quad (10)$$

where  $M_C$  and  $M_D$  are the model orders and  $c_{m,n}$  and  $d_{m,n}$  are the model parameters. The number of parameters in the vorticity and divergence field models are  $N_C = (M_C + 1)(M_C + 2)/2$  and  $N_D = (M_D + 1)(M_D + 2)/2$ , respectively. While the model orders can be selected at will, we have found, based on simulations, that  $M_C = M_D = 2$  is typically adequate for wind estimation.

To solve Eqs. (4), (5) and (7) through (10), these equations are discretized on an  $N \times N$  equally-spaced grid with spacing  $h = 25$  km over the desired region  $\mathcal{L}$ . This corresponds to the 25 km sampling resolution of the wind scatterometer. While  $N = 24$  will cover the entire swath width, the swath can be segmented into smaller regions to reduce  $N$  and the corresponding computational requirements. The pressure and velocity potential fields can be eliminated from the discretized system of equations and the velocity field can be written directly in terms of the pressure field boundary conditions and the parameters of the vorticity and divergence fields. The resulting equation relating the velocity component fields to pressure field boundary conditions and the vorticity and divergence model parameters can be expressed, as (Ref. 12)

$$\begin{bmatrix} \bar{U} \\ \bar{V} \end{bmatrix} = F \bar{X}. \quad (11)$$

where the  $N^2$  element vector  $\bar{U}$  is the lexicographic-ordered  $u$  component wind field at grid sample points,  $\bar{V}$  is the lexicographic ordered  $v$  component wind field, and, the  $\bar{X}$  vectors contains  $4N - 2$  pressure field boundary conditions and  $N_C + N_D$  vorticity and divergence field parameters. The full-rank rectangular matrix  $F$  consists of known constants.

Equation (11) provides a parametric wind field model which relates the model parameters (in  $\bar{X}$ ) to the wind field (in  $\bar{U}$  and  $\bar{V}$ ). This wind field model easily lends itself to the parameter estimation formulation: the model parameters in  $\bar{X}$  are directly estimated from the noisy  $\sigma^c$  measurements and the wind field is then computed from the parameters using Eq. (11).

### 6. WIND FIELD MODEL EVALUATION

To evaluate our model formulation we have used simulated mesoscale wind fields since little conventional oceanic mesoscale data is available (Ref. 5). The test wind fields were generated by state-of-the-art numerical weather prediction techniques at 1.875 deg resolution. The fields were interpolated to 10 km and small-scale variability with a  $k^{-2}$  spectrum (Ref. 7) was added. The wind fields were selected to span a wide range of meteorological conditions.

To test the vorticity and divergence model order, a grid size  $N$  was selected and the modelling error evaluated for different model orders  $M_C$  and  $M_D$ . The modeling error was computed

as follows. At a given location, the model parameters  $\bar{X}$  were computed, by

$$\hat{\bar{X}} = (F^T F)^{-1} F^T \begin{bmatrix} \bar{U} \\ \bar{V} \end{bmatrix}. \quad (12)$$

The model wind field computed from these parameters, is

$$\begin{bmatrix} \widehat{U} \\ \widehat{V} \end{bmatrix} = F \hat{\bar{X}}. \quad (13)$$

The RMS errors (vector, speed, and direction) between the true field and the model field were computed. To limit the computation required, the swath was segmented to permit the use of various  $N$  values. The errors reported below are the RMS over all segments of the wind fields. The results for  $N = 12$  (a  $300 \times 300$  km region  $\mathcal{L}$ ) and various  $M_C$  and  $M_D$  are shown in Table 1. The effects of varying  $N$  but holding  $M_C$  and  $M_D$  fixed are illustrated in Table 2.

For a fixed  $N$ , as the model orders are increased, the RMS errors decrease and the number of unknowns grows. Values of  $M_D = M_D = 1$  or  $M_D = M_D = 2$  keep the number of unknowns small while providing adequate accuracy for wind field estimation. From Table 2 we see that for fixed  $M_D$  and  $M_C$  the RMS error increases with  $N$ . While the number of unknowns also grows with  $N$ , the total number of swath segments also decreases. We have found that both  $N = 8$  and  $N = 12$  are suitable for wind estimation. Larger values of  $N$  can be used but require more computation to optimize the objective function.

## 7. OBJECTIVE FUNCTION FORMULATION

The scatterometer provides noisy measurements of  $\sigma^\circ$ , which is a non-linear transformation,  $\mathcal{M}$ , of the velocity field. At a given sample point, the  $k^{\text{th}}$  measurement  $z(k)$  of the true  $\sigma^\circ$  value includes additive zero-mean Gaussian noise which has a variance that is a quadratic function of the true  $\sigma^\circ$  (Ref. 6), i.e.,

$$\text{Var}[z(k)] = \alpha^2(k)\sigma^{\circ 2}(k) + \beta^2(k)\sigma^\circ(k) + \gamma^2(k) \quad (14)$$

where  $\alpha(k)$ ,  $\beta(k)$ , and  $\gamma(k)$  are known constants which depend on the observation angle, polarization, and swath location of the measurement. The measurement noise is assumed to be independent for each different measurement of  $\sigma^\circ$ . Disregarding constants, the point-wise log-likelihood function is

$$l(u, v) = - \sum_{k=1}^L \left\{ \ln[\alpha^2(k)\sigma^{\circ 2}(k) + \beta^2(k)\sigma^\circ(k) + \gamma^2(k)] + [z(k) - \sigma^\circ(k)]^2 / [\alpha^2(k)\sigma^{\circ 2}(k) + \beta^2(k)\sigma^\circ(k) + \gamma^2(k)] \right\} \quad (15)$$

where  $L$  is the number of available  $\sigma^\circ$  measurements at the sample point and  $\sigma^\circ(k)$  is related to the components  $(u, v)$  of the wind vector by the geophysical model function  $\mathcal{M}$ , i.e.,

$$\sigma^\circ(k) = \mathcal{M}\{(u, v), k\}. \quad (16)$$

In the traditional point-wise approach, the values of  $(u, v)$  which maximize the log-likelihood function in Eq. (15) are the ambiguity set for the sample point.

In the model-based approach, we estimate the wind field model parameter vector  $\bar{X}$  directly from the noisy  $\sigma^\circ$  measurements and then compute the velocity fields from the estimated model parameter vector. For our wind field model, formulation of the field-wise objective function (based on either maximum-likelihood or least-squares criteria) for the model parameters ( $\bar{X}$ ) is straight forward. Disregarding constants, the log-likelihood function for  $\bar{X}$  can be written, as

$$l(\bar{X}) = - \sum_{i=1}^N \sum_{j=1}^N \sum_{k=1}^{L_{i,j}} \left\{ \ln[\alpha_{i,j}^2(k)\sigma_{i,j}^{\circ 2}(k) + \beta_{i,j}^2(k)\sigma_{i,j}^\circ(k) + \gamma_{i,j}^2(k)] + [z_{i,j}(k) - \sigma_{i,j}^\circ(k)]^2 / [\alpha_{i,j}^2(k)\sigma_{i,j}^{\circ 2}(k) + \beta_{i,j}^2(k)\sigma_{i,j}^\circ(k) + \gamma_{i,j}^2(k)] \right\} \quad (17)$$

where  $\sigma_{i,j}^\circ(k)$  is the value of  $\sigma^\circ$  obtained by evaluating the wind field model at  $\bar{X}$  and using the  $u$  and  $v$  components of the wind vector at the grid point  $(i, j)$  in the  $\mathcal{M}$  function, i.e.,

$$\sigma_{i,j}^\circ(k) = \mathcal{M}\{(F\bar{X})_{i,j}, k\} \quad (18)$$

The field-wise objective function is the negative of the field-wise log-likelihood function. The value of  $\bar{X}$  which minimizes the field-wise objective function is the maximum likelihood estimate of  $\bar{X}$ . The estimated wind field is computed from  $\bar{X}$ .

Due to the complicated nature of the field-wise objective function we must resort to numerical techniques. Unfortunately, the dimensionality of the minimization is rather high (there are  $4N - 2 + N_C + N_D$  model parameters in  $\bar{X}$ ). Numerical minimization of the objective function is difficult due to the nature of the objective function which inherits its properties from the nature of  $\mathcal{M}$ . The harmonic form of  $\mathcal{M}$  gives rise to (a) numerous local minima, and (b) the potential for multiple global minima in the objective function. While it is possible to have multiple global minima, which would give rise to multiple field estimates, we have not observed this in our testing. In the event that multiple minima should occur, selecting a single solution for the field-wise case is much simpler than for the point-wise case, since the ambiguity can readily be resolved by comparison with adjacent swath segments.

## 8. COMPARISON OF APPROACHES

The comparisons we have made between our model-based approach and the traditional point-wise approach indicate that our approach yields significantly more accurate wind field estimates *even when perfect dealiasing is assumed* (i.e., the ambiguity closest to the true wind is used as the dealiased wind). The point-wise approach can never do better. This comparison was made using simulated NSCAT data and includes the effects of communication noise, imperfect  $\sigma^\circ$  cell coregistration, and geophysical modeling errors in  $\mathcal{M}$ .

To illustrate the performance difference, consider Figs. 1-3. For this example  $N = 8$  and  $M_C = M_D = 2$ . Fig. 1 shows a  $300 \times 300$  km region of the true mesoscale wind field, sampled at 25 km resolution, in solid vectors. The broken vectors show the wind field resulting from fitting the model to the true wind field. Fig. 3 shows the ambiguous solution sets obtained using the point-wise estimation approach on the simulated  $\sigma^\circ$  measurements. The solid vector indicates the closest ambiguity to the true wind field. A wind field consisting of these closest ambiguities would be the result of "perfect dealiasing". Note that point-wise solution sets are not present at some sample points. This is due to the fact that for adequate point-wise wind estimation, at least one  $\sigma^\circ$  measurement from each of the antenna beams is required. Instrument calibration cycles and  $\sigma^\circ$  cell coregistration errors result in missing measurements at some sample points in the swath. At these sample points, no wind can be estimated using the point-wise approach. Fig. 2 illustrates the results obtained using our model-based estimation approach applied to the same  $\sigma^\circ$  measurements. These results should be compared to the solid vectors of Fig. 1. The model-based approach does not suffer from the limitation of requiring a full compliment of  $\sigma^\circ$  measurements at each sample point, but is able to obtain wind estimates for each point of the wind field. Note that the model-based wind field estimate is much less "noisy" than the point-wise closest ambiguity wind field. A comparison of the RMS difference between the true wind field and the estimated wind fields for both cases is shown in Table 3.

## 9. SUMMARY

The traditional approach to solving the wind estimation problem leads to multiple solutions requiring *ad hoc* dealiasing techniques to produce a unique solution. We have introduced a model-based estimation technique which, by imposing a model on the underlying wind field, eliminates this error-prone dealiasing step and yields more accurate estimates of the wind *even when perfect dealiasing is assumed*. In our approach, the noisy wind scatterometer measurements are used to estimate the parameters of the wind field model. The improved performance can be attributed to the fact that the model-based approach takes advantage of the inherent correlation between the wind at different sample points to reduce the noise in the final wind estimates.

## 10. REFERENCES

1. Anderson D et al 1987, *A Study of the Feasibility of Using Sea and Wind Information from the ERS-1 Satellite - Part 1: Wind Scatterometer Data*, ESRIN Contract Report, 6297/86/HGE-1(SC).
2. Atlas R et al 1987, *Global Surface Wind and Flux Fields from Model Assimilation of Seasat Data*, *Journal of Geophysical Research*, Vol 92, No C6, 6477-6487.

3. Bijlsma S J et al 1986, Computation of the Streamfunction and Velocity Potential and Reconstruction of the Wind Field, *Monthly Weather Review*, No 114, 1547-1551.
4. Bracalente E et al 1980, The SASS Scattering Coefficient ( $\sigma_0$ ) Algorithm, *IEEE Journal of Oceanic Engineering*, Vol OE-5, No 2, 145-154.
5. Brown R A and Levy G 1986, Ocean Surface Pressure Fields from Satellite-Sensed Winds, *Monthly Weather Review*, Vol 114, No 11, 2197-2204.
6. Chi C-Y et al 1986, Radar Backscatter Measurement Accuracies Using Digital Doppler Processors in Spaceborne Scatterometers, *IEEE Trans on Geoscience and Remote Sensing*, Vol GE-24, No 3, 426-437.
7. Freilich M H 1986, Satellite Scatterometer Comparisons with Surface Measurements: Techniques and SEASAT Results", *Proc of a Workshop on ERS-1 Wind and Wave Calibration*, June 1986, ESA SP-262, 57-62.
8. Freilich M H and Chelton D B 1986, Wavenumber Spectra of Pacific Winds Measured by the Seasat Scatterometer, *Journal of Physical Oceanography*, Vol 16, No 4, 741-757.
9. Hoffman R N 1982, SASS Wind Ambiguity Removal by Direct Minimization, *Monthly Weather Review*, Vol 110, 434-445.
10. Hoffman R N 1982, SASS Wind Ambiguity Removal by Direct Minimization. Part II: Use of Smoothness and Dynamical Constraints, *Monthly Weather Review*, Vol 112, 1829-1852.
11. Li F et al 1964, NROSS Scatterometer - An Instrument for Global Oceanic Wind Observations, *Proc SPIE*, Arlington, Virginia, May 3-4, Vol 481, 193-197.
12. Long D 1988, *Wind Field Modeling*, USC Internal Report, April 18.
13. Lynch P 1988, Deducing the Wind from Vorticity and Divergence, *Monthly Weather Review*, Vol 116, 86-93.
14. Schroeder L et al 1985, Removal of Ambiguous Wind Directions for a Ku-band Wind Scatterometer Using Measurements at Three Different Azimuth Angles, *IEEE Trans on Geoscience and Remote Sensing*, Vol GE-23, No 2, 91-100.
15. Ulaby F T et al 1981, *Microwave Remote Sensing*, In three volumes, Addison-Wesley Pub Co, Reading, Mass.
16. Wurtele M G et al 1982, Wind Direction Alias Removal Studies of SEASAT Scatterometer-Derived Wind Fields, *Journal of Geophysical Research*, Vol 87, No C5, 3365-3377.

Table 1: Wind Field Modeling Error - ( $N = 12$ )

Model Order		RMS Error		
$M_C$	$M_D$	Vector Magnitude (m/s)	Direction (deg)	Speed (m/s)
0	0	0.123	6.256	0.082
0	1	0.111	5.725	0.074
0	2	0.107	5.502	0.071
0	3	0.105	5.445	0.069
0	4	0.105	5.373	0.070
1	0	0.108	5.591	0.070
1	1	0.094	4.914	0.060
1	2	0.089	4.658	0.057
1	3	0.088	4.566	0.056
1	4	0.089	4.617	0.057
2	0	0.104	5.397	0.067
2	1	0.089	4.666	0.056
2	2	0.085	4.378	0.053
2	3	0.083	4.289	0.052
2	4	0.083	4.277	0.052
3	0	0.103	5.357	0.066
3	1	0.088	4.623	0.056
3	2	0.084	4.331	0.052
3	3	0.083	4.237	0.051
3	4	0.082	4.207	0.051
4	0	0.102	5.374	0.066
4	1	0.087	4.580	0.056
4	2	0.081	4.227	0.051
4	3	0.082	4.263	0.052
4	4	0.083	4.439	0.053

Table 2: Wind Field Modeling Error - ( $M_C=M_D=2$ )

$N$	RMS Error		
	Vector Magnitude (m/s)	Direction (deg)	Speed (m/s)
4	0.04	1.49	0.02
6	0.08	3.18	0.05
8	0.09	3.76	0.05
12	0.09	4.38	0.05

Table 3: RMS difference between the estimated and true fields

Wind Estimation Approach	RMS Error		
	Vector Magnitude (m/s)	Direction (deg)	Speed (m/s)
Point-wise	1.3	15.1	0.44
Model-based	0.9	7.3	0.68

Figure 1: True wind field (solid), model wind field (dotted).

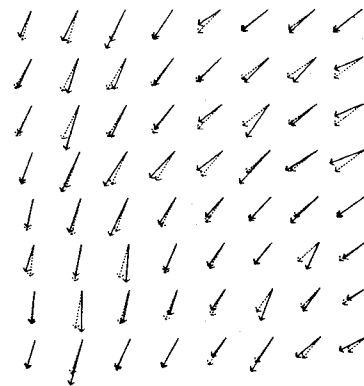


Figure 2: Model-based wind field estimate.

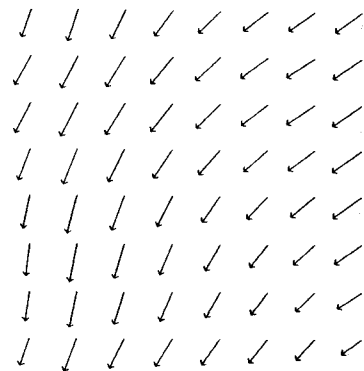


Figure 3: Point-wise ambiguities.

